SCANNING VOL. 36, 384–393 (2014)

Performance of SEM Scintillation Detector Evaluated by Modulation Transfer Function and Detective Quantum Efficiency Function

Jan Bok and Petr Schauer

Institute of Scientific Instruments of the ASCR, Brno, Czech Republic

Summary: In the paper, the SEM detector is evaluated by the modulation transfer function (MTF) which expresses the detector's influence on the SEM image contrast. This is a novel approach, since the MTF was used previously to describe only the area imaging detectors, or whole imaging systems. The measurement technique and calculation of the MTF for the SEM detector are presented. In addition, the measurement and calculation of the detective quantum efficiency (DQE) as a function of the spatial frequency for the SEM detector are described. In this technique, the time modulated e-beam is used in order to create well-defined input signal for the detector. The MTF and DQE measurements are demonstrated on the Everhart–Thornley scintillation detector. This detector was alternated using the YAG:Ce, YAP:Ce, and CRY18 single-crystal scintillators. The presented MTF and DQE characteristics show good imaging properties of the detectors with the YAP:Ce or CRY18 scintillator, especially for a specific type of the e-beam scan. The results demonstrate the great benefit of the description of SEM detectors using the MTF and DQE. In addition, point-by-point and continual-sweep e-beam scans in SEM were discussed and their influence on the image quality was revealed using the MTF. SCANNING 36:384–393, 2014. © 2013 Wiley Periodicals, Inc.

Key words: MTF, DQE, image detection, scintillator, e-beam scanning

Contract grant sponsor: Technology Agency of the Czech Republic; Contract grant number: TE01020118; Contract grant sponsor: Czech Science Foundation; Contract grant number: P102/10/1410; Contract grant sponsor: European Commission and the Ministry of Education, Youth, and Sports of the Czech Republic. Contract grant number: EE.2.3.20.0103.

*Address for reprints: Jan Bok, Institute of Scientific Instruments of the ASCR, v.v.i., Kralovopolska 147, 612 64 Brno, Czech Republic
E-mail: bok@isibrno.cz

Received 23 September 2013; Accepted with revision 10 November 2013

DOI: 10.1002/sca.21130
Published online 3 December 2013 in Wiley Online Library (wileyonlinelibrary.com).

Introduction

The images in SEM are formed by a process composed of several steps. In the first step, the e-beam is scanned across an object with certain precision of the scan and the signal-electrons are produced. These electrons, representing intensity of one image pixel, are emitted from an area given by the e-beam current profile and its interaction volume. In the next step, the signal-electrons are collected and converted to the electrical signal with certain efficiency by the detector. At the end of the process, the signal is formed to the digital image using the analog-to-digital conversion. All the steps can influence the quality of the resulting image and efforts are made to evaluate them in context of the image quality. Because the influence of the SEM detector on the image quality is frequently neglected, we aimed to show that the detector's influence can be considerable. Thus, this paper is focused on only one step of the image formation process, which is the signal-electron conversion to the analog electronic signal by the SEM detector. A novel method how to evaluate the influence of only the separate detector is described below.

One of the most crucial features of a SEM electron detector is its time dependent reaction to the incoming signal pulse, called the time response. A short time response is important, since fast e-beam scanning is often demanded in SEM. If the detector response is slower than the scan, the image is blurred and the image contrast is reduced. The detector response is usually described by the time-dependent rise and decay characteristics of the detector output signal as a reaction to the incident single electron, or electron pulse (Novák and Müllerová, 2009). Usually, these characteristics have a more complex form, such as the multi-exponential function of time. Therefore, the evaluation and comparison of the time-dependent characteristics in the context of their influence on the image quality can be rather complicated.

This paper proposes to evaluate the detector response using the modulation transfer function (MTF). This function describes how faithfully an imaging system reproduces (or transfers) contrast from the object to the

image. The MTF is expressed as a function of the spatial frequency, which gives the information about the contrast transfer at a certain level of the image detail. The MTF, or similarly the contrast transfer function (CTF), is used to describe various imaging systems, including electron microscopes. In the past, the MTF and CTF was measured and calculated for transmission electron microscopes (Mitome, '99; Danov *et al*., 2000; Mallick *et al*., 2005; Sorzano *et al*., 2007) and also for scanning electron microscopes (Joy *et al*., 2010; Griffin, 2011). Besides the measurement of the complex imaging systems, the MTF was also used to describe the area imaging detectors, such as photographic films, luminescent screens, CCD and CMOS sensors (Boreman, 2001). In electron microscopy, the MTF for the area electron detectors was reported (Van Zwet and Zandbergen, '96; Zuo, '96; Horacek, 2005; Faruqi and Henderson, 2007; McMullan *et al*., 2009a).

The area imaging detectors capture the area distribution of the signal intensity at the same moment. Contrary to the area detectors, the SEM detectors capture the signal intensity as a time sequence during the scanning. Such detectors can be called point imaging detectors because they obtain the signal only from one point of the object at the same moment. Although the contrast transfer of the area detectors is usually described by the MTF, the point detectors were never described in such a way. The reason is the apparent impossibility of evaluating the contrast transfer of the point detector if it does not detect the signal in the space coordinates. However, it will be shown in this paper that the mathematical apparatus of the MTF can also be expanded on the field of such detectors and this description can bring great benefits.

Another important parameter of the SEM detector is its signal-to-noise ratio (SNR). The output SNR compares the level of the desired signal to the level of noise. The output SNR is not comparable among different detectors because the noise includes not only the noise caused by the detector but also the background noise of the input signal. For the comparison of the output signal and the noise produced by the detector only, the detective quantum efficiency (DQE) is used. Since the DQE is defined as the ratio of the squared output SNR to the squared input SNR, it gives information about how the available SNR is degraded by the detector. Together with the time response of the detector, the DQE affects the image contrast and therefore higher DQEs are always demanded.

Analogous to the MTF, the DQE is generally expressed as a function of the spatial frequency, and therefore, it is used to describe the area imaging detectors. Measurement of the DQE of the area electron detectors in electron microscopy was reported previously (Taniyama *et al*., '97; Meyer and Kirkland, 2000; Faruqi and Henderson, 2007; McMullan *et al*., 2009b; Milazzo *et al*., 2010). The DQE for the point imaging detectors was also measured (Browne and Ward, '82; Joy *et al*., '96; Oatley, 2004); however, it was not expressed as a function of the spatial frequency, but only as the limit as the spatial frequency approaches zero. The DQE of the SEM detector as a function of the spatial frequency has never been presented before. Therefore, another aim of this paper is to show that the SEM detector can be also described by the spatial-frequency dependent DQE function, the same as the area detector. The DQE function can give more information about the SEM image properties than was available before.

The MTF and DQE measurement and calculation were carried out on the Everhart–Thornley scintillation detector, which is the most common type of the SEM detector for the secondary electron detection. This detector consists of a collector grid, metal-coated scintillator, light-guide, photomultiplier tube (PMT), and amplifier (Everhart and Thornley, '60). The detected secondary electrons are attracted by the grid and accelerated towards the scintillator typically to the energy of 10 keV. The detector used in our experiment was alternated with the YAG:Ce, YAP:Ce, and CRY18 single-crystal scintillators which are frequently used in modern Everhart–Thornley detectors. The light-guide, PMT and amplifier stayed unchanged. The reason of our choice was to show the considerable influence of the scintillator on the MTF and DQE when the e-beam scanning is as fast as the detector response (Joy *et al*., '96; Schauer, 2011).

Methods

Modulation Transfer Function

In SEM, an object is scanned by the e-beam with two sets of deflector coils. The coil corresponding to the deflection along the horizontal image axis is supplied with the staircase, or sawtooth voltage waveform. The staircase waveform provides a point-by-point e-beam scan, whereas the ramp part of the sawtooth waveform provides a continual-sweep scan. Choice of the scan type influences the image quality, as will be shown later. The following considerations are simplified by assuming only the scan along the horizontal axis. The e-beam movements to the next horizontal line are not assumed. These movements along the vertical axis take no more than 1% of the total scanning time and thus they will be neglected for simplification.

Suppose that the intensity distribution in the object is described by the function $o(x)$. Similarly, the e-beam current distribution is described by $p(x)$. In the case of the point-by-point scan (PBP), the input signal $i_{\mathrm{in}}(t)$ incoming from the object to the SEM detector, is given by the step function containing the product of the intensity distribution $o(x)$ with the e-beam profile $p(x)$ at each possible position given by $n\lambda$:

$$i_{\text{in}}^{\text{PBP}}(t) = \sum_{n=0} \chi_{[n\tau,(n+1)\tau)}(t) \int_{\text{obj}} o(x)p(x - n\lambda)\,\mathrm{d}x \qquad (1)$$

where n is number of the pixel, λ is the object distance corresponding to one pixel and τ is the dwell time corresponding to the period of one pixel integration. Higher dwell time corresponds to slower e-beam scan and vice versa. The function $\chi_{[n\tau,(n+1)\tau)}(t)$ is the indicator function having the value 1 for t in the interval $[n\tau, (n+1)\tau)$ and the value 0 for t not in this interval. The purpose of this function is to transfer the signal to the time scale. In the case of the continual-sweep scan (CS), the input signal is given by the convolution of the functions $o(x)$ and $p(x, t)$; the indicator function is not presented:

$$i_{\text{in}}^{\text{CS}}(t) = (o^{*}p)(t) = \int_{\text{obj}} o(x)p(x - (\lambda/\tau)t)\,\mathrm{d}x \qquad (2)$$

The previous equations express the time-variable signal incoming to the detector. This input signal is then distorted by the detector time response, which can be expressed as a function of time $r(t)$. The output signal $i_{\text{out}}(t)$ outgoing from the detector is given by the convolution of the input signal with the time response:

$$i_{\text{out}}(t) = r(t)^{*} i_{\text{in}}(t) \qquad (3)$$

In order to obtain the digital sequence of the pixels, the analog output signal is digitalized by the signal sampling and reconstruction (Pratt, 2006). This process can be characterized by the linear conversion of the time dependent signal to the space dependent image signal. It can be expressed as a transformation of the coordinates:

$$x = \tau^{-1} t \qquad (4)$$

Using this transformation, the time response $r(t)$ can be treated as the so-called space response $r(x)$ which causes a decrease of the spatial contrast.

In order to test the SEM image contrast, one can scan an object consisting of a grid of electron-emitting (white) and non-emitting (black) lines and observe the resulting image. The number of alternations from the black line to the white line per image distance represents the level of detail and it is called spatial frequency. Higher spatial frequencies generally correspond to fine details, low frequencies represent global information about the shape. The spatial frequency is often expressed in units of line pairs per object distance, but in digital systems it is more convenient to use units of line pairs per pixel (lp/pixel), since the pixel size corresponds to some object distance.

The measure of the system's ability to transfer the contrast from the object to the image in dependence on spatial frequency is the modulation transfer function (MTF), or the contrast transfer function (CTF). The MTF and the CTF are defined similarly; however, the MTF uses the sine wave variations from black to white, instead of the square wave as in the case of the CTF (Pavan *et al.*, '93). From the theory of the imaging systems, it arises that the MTF equals the magnitude of the Fourier transform of the system's space response $r(x)$ (Williams, '98). In order to obtain an equation for the MTF, one must use the convolution theorem which says that the Fourier transform of the convolution equals the product of the Fourier transforms (Bracewell, '99). Then Equation (3) can be rewritten as

$$I_{\text{out}}(f) = \text{MTF}(f) I_{\text{in}}(f) \qquad (5)$$

where I_{out}, I_{in}, and MTF are the Fourier transforms of i_{out}, i_{in}, and r, respectively.

Since the MTF is a function of spatial frequency, it is used for characterization of the area detectors, because they detect the signal in the space domain. The novel approach is to use the transformation in Equation (4), which enables to convert the time response to the space response. Therefore, the MTF can be used to describe not only area detectors, but also the point detectors detecting the signal in the time domain, such as the SEM detectors. Since the time coordinate can be linearly transformed to the space coordinate, similarly the temporal frequency f can be transformed to the spatial frequency s according to $s = \tau f$. Then from Equation (5), the MTF can be expressed in the space frequency coordinate and normalized by the term of $I_{\text{in}}(0)/I_{\text{out}}(0)$ as

$$\text{MTF}_{\tau}(s) = \frac{I_{\text{in}}(0)}{I_{\text{out}}(0)} \frac{I_{\text{out}}(s)}{I_{\text{in}}(s)} \qquad (6)$$

It follows from Equation (6) that the MTF calculation is based on the knowledge of the time-varying detector input and output signal. The input signal in SEM is represented by the current of the electrons reflected/emitted by an arbitrary object. The output signal is represented by the voltage of the detector output. Although the voltage can be easily measured by an oscilloscope, the measurement of low time-varying current of the electrons is a problematic task, since the time response of a measuring device will always distort the weak signal. One of the solutions is to generate the periodically varying current of the incident electrons and to measure only the mean of the current. The generation of the periodic current can be done by positioning the detector directly against the time modulated e-beam instead of obtaining the reflected electrons from the object. The e-beam can be modulated, for instance, by the periodic e-beam blanking (deflection outside and inside an aperture).

The generated e-beam current must be correlated with an imaginary object which contains the information

about the space domain. Therefore, the imaginary object has to be defined first and then the e-beam current can be generated according to the object. The most comprehensive object is a grid consisting of the white and black lines (see Fig. 1a). Its contrast profile $o(x)$ is described by the square wave with the value 1 in the interval $[2k\lambda, (2k+1)\lambda]$ (where $k \in Z$) representing one bright pixel and with the value 0 not in the mentioned interval (see Fig. 1b). The e-beam profile $p(x)$ can be approximated as a square waveform of the pixel size (the value 1 in the interval $[0, \lambda]$). Substituting $o(x)$ and $p(x)$ in Equations (1) and (2), the required e-beam current $i'_{\text{in}}(t)$ is obtained for the point-by-point scan (Fig. 1c):

$$i_{\text{in}}^{\text{PBP}'}(t) = \sum_{n=0} \chi_{[2n\tau,(2n+1)\tau)}(t) \tag{7}$$

and for the continual-sweep scan (Fig. 1d):

$$i_{\text{in}}^{\text{CS}'}(t) = \sum_{n=0} \left[(-1)^{n+1}(\tau^{-1}t - (n+0.5)) + 0.5\right] \chi_{[n\tau,(n+1)\tau)}(t) \tag{8}$$

It follows from Equation (7) that the input signal of the incident electrons $i_{\text{in}}^{\text{PBP}'}(t)$ can be generated by the e-beam un-blanking for the period given by the dwell time τ. In the case of $i_{\text{in}}^{\text{CS}'}(t)$, the generation of the e-beam current is rather complicated, since the current should have the form of the time dependent triangle wave.

Detective Quantum Efficiency

The detective quantum efficiency (DQE) is defined as:

$$\text{DQE}(s) = \frac{\text{SNR}_{\text{out}}^2(s)}{\text{SNR}_{\text{in}}^2(s)} \tag{9}$$

where $\text{SNR}_{\text{in}}^2(s)$ and $\text{SNR}_{\text{out}}^2(s)$ are the quadratic spectral signal-to-noise ratios for the input and the output signal, respectively (Jones, '59; Unser *et al.*, '87). The quadratic spectral SNR is defined as the ratio of the Fourier transform of the signal and noise:

$$\text{SNR}^2(s) = \frac{\text{FT}^2(\text{signal})}{\text{FT}^2(\text{noise})} \tag{10}$$

where the signal and noise are taken to be calibrated in terms of the signal-electrons. Also, it is supposed that the detector is linear and the imaging performance is the same during the measurement (Cunningham and Shaw, '99). Thus, the DQE function is a measure of how the signal-to-noise ratio is degraded by the imaging system at the different spatial frequencies. The DQE is

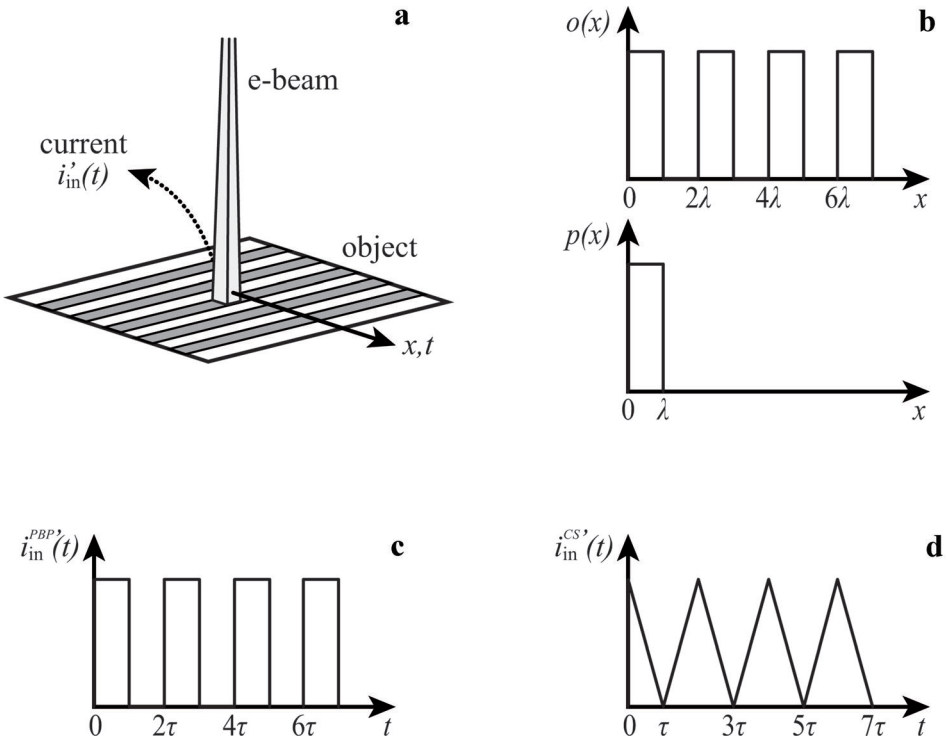

Fig 1. (a) The approximation of the e-beam scanning across the object. (b) Assuming that the object intensity distribution is $o(x)$ and the e-beam current has distribution $p(x)$, the time-varying signal $i'_{\text{in}}(t)$ incoming to the detector has well-defined form for (c) the point-by-point scan and for (d) the continual-sweep scan.

always less than unity and therefore it shows how efficiently the imaging system detects the input signal as compared to the ideal detector.

The novel approach is to measure the DQE for a SEM detector as a function of the spatial frequency. Equation (10) can be used for the formulation of the expression for the SNR_{in} of the SEM detector:

$$SNR_{in}^2(s) = \frac{FT^2(i_{in})}{FT^2(noise_{in})} = \frac{I_{in}^2(s)}{NPS_{in}(s)} \tag{11}$$

Similarly, the equation for the SNR_{out} is written from Equation (10) using Equation (6):

$$SNR_{out}^2(s) = \frac{FT^2(i_{out})}{FT^2(noise_{out})} = \frac{I_{out}^2(s)}{NPS_{out}(s)} = \frac{I_{out}^2(0)}{I_{in}^2(0)} \frac{MTF^2(s) I_{in}^2(s)}{NPS_{out}(s)} \tag{12}$$

The $NPS_{in}(s)$ and $NPS_{out}(s)$ stands for the noise power spectra defined as the quadrate of the Fourier transform of the uniform input or output signal, respectively. The uniform input signal is represented by the non-modulated e-beam current. In the case of low current, the input signal is assumed to be the uniform Poisson distribution and therefore $NPS_{in} = I_{in}$. The uniform output signal is obtained from homogeneously illuminated pixels and it is sampled with the frequency identical to the double of the Nyquist frequency, which corresponds to the sample interval equal to the dwell time.

Substituting the terms in Equation (9) with Equations (11) and (12), the final expression for the DQE is:

$$DQE(s) = G \frac{MTF^2(s) I_{in}(s)}{NPS_{out}}(s) \tag{13}$$

where $G = I_{out}^2(0)/I_{in}^2(0)$ is the detector gain. The DQE is thus calculated using the previously obtained MTF and I_{in}, and the only addition is the measurement of the NPS_{out}.

Experimental

The MTF and DQE were measured and calculated for the Everhart–Thornley scintillation detector. The detector used in our experiments was alternated with four specimens of the scintillators (the light-guide, PMT, and amplifier stayed unchanged). The single crystal scintillators were produced by CRYTUR, Ltd. and they were coated with a 50 nm thin aluminium layer. The specimens of the scintillators were chosen as follows: (1) standard YAG:Ce #1; (2) YAG:Ce #2 with low concentration of defect centers; (3) YAP:Ce; (4) CRY18. These scintillation materials are frequently used in modern Everhart–Thornley detectors. The two types of YAG:Ce scintillator were chosen in order to show the influence of the scintillation material defect centers on the response of the detector. The PMT was Tesla 65-PK-415 and the amplifier was Hamamatsu C9663.

The detectors were tested using a device built in our laboratory (Bok and Schauer, 2011). In this device (Fig. 2), the scintillator was attached to the front of the fused-silica light-guide and it was positioned directly against the focused electron beam with the energy of 10 keV and with the variable current up to 50 μA. The e-beam was modulated by electrostatic deflectors located above an aperture. The deflectors were supplied by the square waveform from the pulse generator EMG TR-0331. The deflection system was able to produce the e-beam pulses of the variable width (the minimum was 50 ns) having the 800 ps rise and fall time (measured in the range of 10–90% of the e-beam current intensity). In order to measure the incident e-beam current, a Faraday cage was connected to the scintillator and located around it. The Faraday cage current was converted to the voltage and sampled by the Agilent 34401A multimeter. The light signal from the scintillator was carried out from the chamber by the light-guide to the PMT photocathode. The detector output signal was recorded using the 2.5 GHz oscilloscope Tektronix DPO7254.

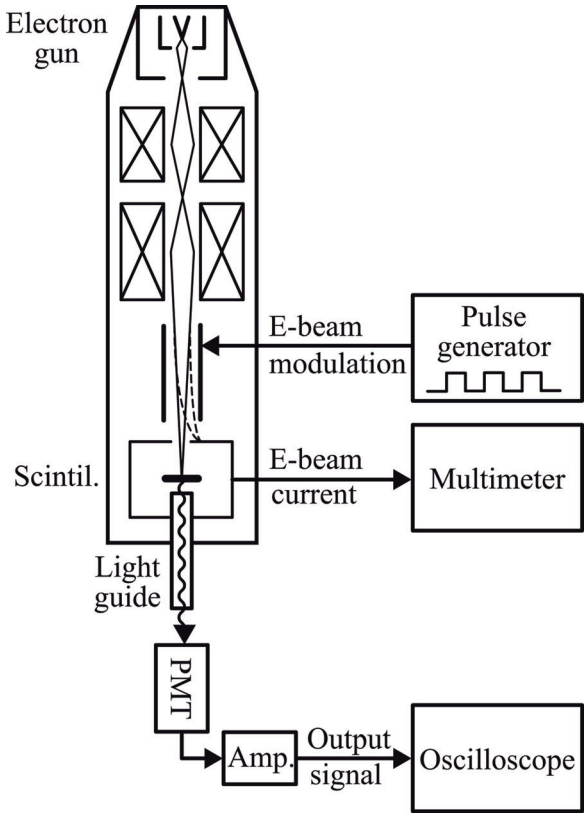

Fig 2. The schematic diagram of the device built in our laboratory for testing Everhart–Thornley detectors.

The detector input signal was generated by the e-beam with the defined current and modulated according to Equation (7). Here, the e-beam current has a square waveform with the duty cycle of 50% and with the pulse duration equal to the dwell time. The time response of the oscilloscope, including the connections, was neglected. In order to obtain the NPS, the output noise signal was measured using the oscilloscope in the long time scale during the non-modulated e-beam current. The NPS curve was spline interpolated because the NPS curve was noisy, and thus it was difficult to obtain the exact number for low frequencies.

Results and Discussion

The square electron current pulse with the duration of 100 ns was generated in order to test the time response of the mentioned alternatives of the SEM detector. The diameter of the e-beam spot was set to 1 mm and the current on the front of the scintillator was 0.79 nA giving the current density of $10^{-7}\,\mathrm{A\,cm^{-2}}$. The decay characteristics of the detector output signal were plotted in the semi-logarithmic graph in Figure 3. Here, it can be seen the scintillators have significant influence on the detector response. The detector with the CRY18 scintillator has the lowest signal intensity at the time of 2 μs; however, the detector with the YAP:Ce has the shortest decay time. By analyzing these characteristics, it is rather complicated to conclude which detector is more suitable for the fast scanning, since the observed characteristics do not contain any explicit information about the influence on the image contrast.

The MTF was measured and calculated for the four mentioned scintillator alternatives as shown in Figure 4a. The dwell time was chosen as 100 ns, which approximately corresponds to the TV scan rate when having image with 600×600 pixels. The unity of the

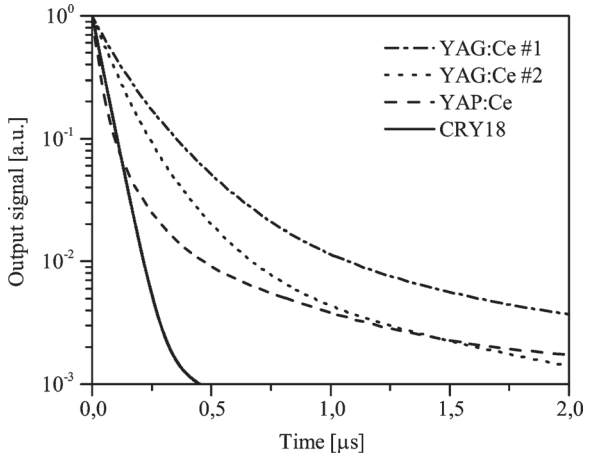

Fig 3. The decay characteristic of the scintillation detector alternatives after the end of a square input pulse with the duration of 100 ns.

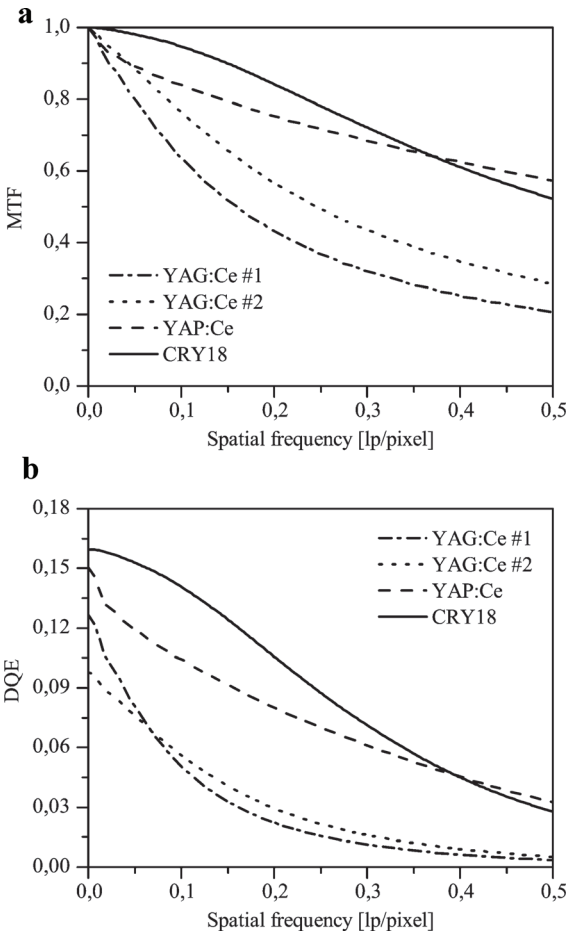

Fig 4. The (a) MTF and (b) DQE of the four alternatives of the scintillators in the tested SEM detector. The dwell time is 100 ns.

MTF represents 100% transfer of the contrast at certain spatial frequency. The MTF characteristic with bigger area under the curve represents a higher mean contrast, and, therefore, it has a better contrast transfer ability for a higher range of the levels of the detail.

The DQE as a function of the spatial frequency was calculated and shown in Figure 4b. Similar to the MTF, the DQE has a bigger area under the curve and that represents lower noise produced by the detector. The calculated DQE(0) has its magnitude at only about 10% of the ideal detector. The reason is that the DQE was decreased mainly by the PMT dark-current noise (which is significantly high in the PMT used), but also by poor lightguide-PMT optical coupling and by the thermal noise of the amplifier used. A comparison of the two YAG:Ce scintillators is noteworthy here. Since the detector with the YAG:Ce #2 has evidently better MTF than the YAG:Ce #1, its DQE for the low spatial frequencies is worse and both the DQE are almost the same for the remaining range of the frequencies. This concludes that not only should the MTF be taken into the consideration, but also the MTF characteristics should be complemented by the DQE function.

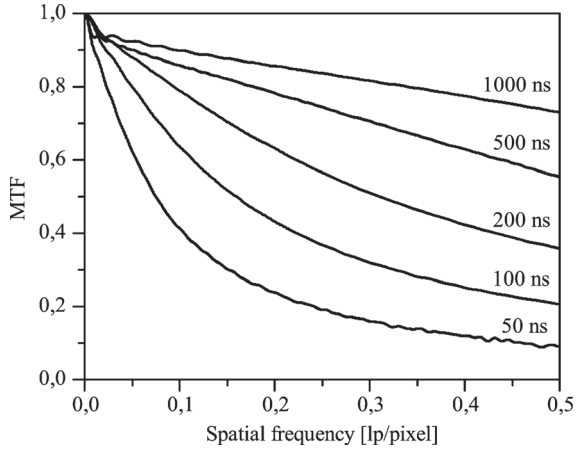

Fig 5. The MTF of the detector using YAG:Ce #1 scintillator for several dwell times.

The influence of the detector time response on the image contrast is more considerable during the fast scanning (smaller dwell times). This is demonstrated in the graph in Figure 5. Here, the MTF was calculated for the detector with the YAG:Ce #1 at several dwell times. The transferred contrast decreases with the decreasing dwell time. The reason is that the decay of the detector signal distorts the information about the adjacent pixels more significantly during the fast scanning.

The question is what scan speed can be used so that the contrast between two pixels will not drop below, for example, 50%. To answer the question, the MTF between two pixels must be obtained. This corresponds to the frequency of 0.5 lp/pixel, because one black-to-white alternation is presented in the distance of 2 pixels. Thus, the MTF and DQE at the frequency of 0.5 lp/pixel were plotted in the semi-logarithmic graph as a function of the dwell time, see Figure 6a,b. It can be seen that the contrast between two pixels increases with increasing dwell time relatively significantly till a certain point, from which it increases slightly. This is a consequence of the multi-exponential form of the detector time response. The minimum dwell time, for which the contrast between two pixels would not drop below 50%, is 380, 200, 65, and 95 ns for the YAG:Ce #1, YAG:Ce #2, YAP:Ce, and CRY18 alternatives, respectively. From the results, it follows that the YAP:Ce scintillator is the most convenient alternative for the very fast scanning when the dwell time is not higher than 100 ns. Nevertheless, the detector with the CRY18 scintillator also has good properties for the fast scanning applications and it has high signal gain. This can be seen in the dependency of the DQE at 0.5 lp/pixel on the dwell time (Fig. 6b), where the gain and noise produced by the detector with CRY18 is evidently the best from the tested detectors.

It must be pointed out that the presented MTF and DQE data were measured and calculated for the ideal point-by-point scan. The comparison of MTFs for point-

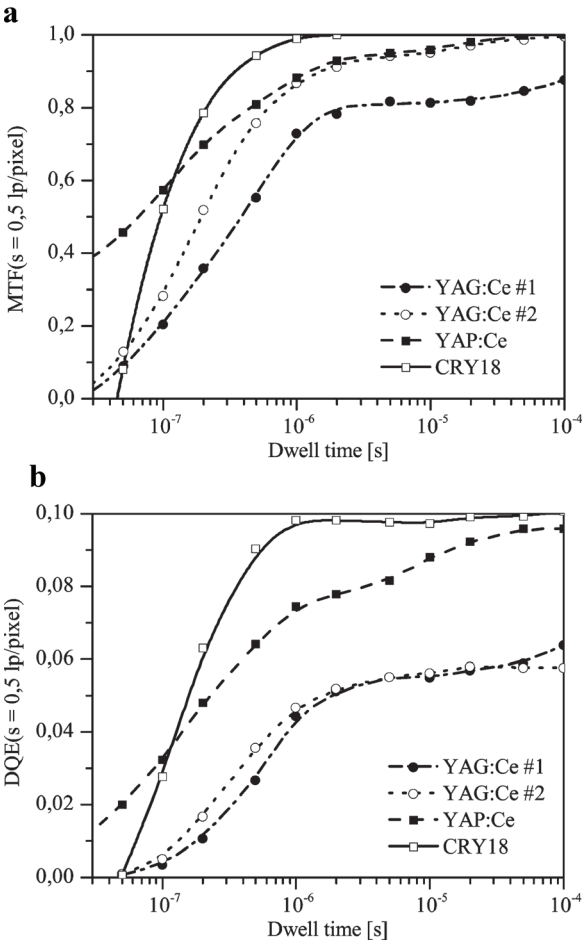

Fig 6. The (a) MTF and (b) DQE of the scintillation detector alternatives at the spatial frequency 0.5 lp/pixel (corresponding to two adjacent pixels) as a function of the dwell time.

by-point and continual-sweep scans is carried out in Figure 7. Here, the MTFs were simulated using the time response of the detector with the CRY18 scintillator. The input signal was obtained from Equations (7)

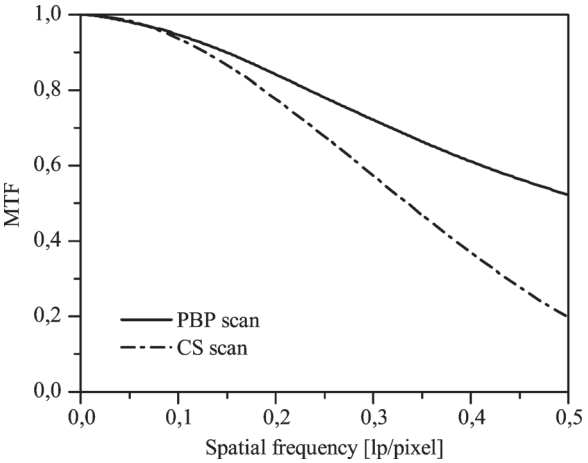

Fig 7. The comparison of the MTF for the point-by-point (PBP) and the continual-sweep (CS) scan. The MTF characteristics are simulated using the time response of the detector with the CRY18 scintillator. The dwell time is 100 ns.

and (8) for point-by-point and continual-sweep scans, respectively. The dwell time was 100 ns. The output signal was not measured, but calculated using Equation (3). The MTF for the continual-sweep scan shows a considerable drop against the point-by-point scan. The reason is that the continual-sweep scan blurs adjacent pixels and their contrast significantly decreases. Therefore, it is recommended to use the point-by-point scan, although this technique is more demanding. The bottleneck of this scan mode is the rise time of the staircase voltage waveform supplying the deflector coils and also the properties of the deflector coils, such as impedance, and capacitance, which slow down the e-beam sweep from one pixel to another. However, this problem can be solved by the electrostatic e-beam blanking while the sweep is performed.

Conclusion

The method for the measurement and calculation of the modulation transfer function (MTF) and the spatial-frequency dependent detective quantum efficiency (DQE) of the point imaging detector, such as the SEM detector, was presented. The measurement method uses the time-modulated e-beam which creates the detector input signal correlated with an imaginary object. This approach gives the information about the detector as it influences the contrast and resolution of the image. The MTF for the detector gives much straightforward information about the detector properties and it can be more suitable than evaluation of the MTF for the whole SEM. The MTF coupled with the DQE for the detector is directly comparable among different detection systems, which is extremely valuable when choosing the detector for particular application.

The method for detector's MTF and DQE measurement was not presented before, thus the discussion of the method accuracy and reliability is necessary. The measurement accuracy is given by the quality of the generated detector input signal and the precision of the output signal measurement. The input signal generated by the modulation (blanking) of the incident e-beam must be stable and the blanking must be much faster than the detector response. In modern electron-optical systems, both requirements are fully satisfied. The time of the e-beam deflection outside the aperture is typically less than half of nanosecond which is two orders shorter than the decay time of the typical SEM detector. Therefore, the modern blanking systems do not decrease the method accuracy. The other problematic part is the measurement of the detector output signal. The measurement is done by an oscilloscope whose sampling frequency should be at least two orders higher than the frequency of the e-beam modulation. Moreover, the dynamic range of the oscilloscope should be at least four orders of magnitude. By fulfilling the described requirements, the measurement error should not exceed units of percent in the whole range of spatial frequencies. Although the measurement error for the MTF and DQE increases with the decreasing spatial frequency, the measured values do not suffer from the considerable inaccuracy.

Since the presented MTF and DQE are measured in the testing device using the modulated e-beam correlated with the imaginary object, it is questionable how accurate this technique is in comparison with the detection of the electrons from the real object. In the Everhart–Thornley detector, the detected secondary electrons are accelerated towards the scintillator typically with the energy of 10 keV. The incident electrons are quasi-monochromatic, they impact whole surface of the scintillator and their mean current is in orders of picoamperes. These conditions are also adjustable in the testing device and then the results are considered to be very reliable as compared to the real situation. However, when dealing with the backscattered electron detectors, where the incident electrons have large energy dispersion, the method cannot be that reliably used. In this case, an approximation must be made in order to handle the non-monochromaticity of the incident electrons.

In the presented method, the three approximations were used to obtain the results and they should be taken into account: (1) The e-beam spot is considered to be homogeneous with the square shape corresponding to the image pixel. This is a rough approximation, since the real e-beam spot has a round shape and its interaction volume can be even larger than the corresponding pixel. Fortunately, this approximation influences markedly the MTF and DQE only at very high spatial frequencies. (2) The method assumes the ideal point-by-point scan. However, the electronics of the deflection coils is not ideal and instead of the immediate e-beam deflection from one point to another, the deflection takes some amount of time. The question is how precisely the point-by-point scan is carried out in SEMs. This feature decreases the MTF and DQE, however it is more significant during the fast scanning (higher dwell times). (3) During the scanning, the e-beam movement to the next horizontal line is not taken into account in the presented method. Since these next-line moves take no more than 1% of the scanning time, the e-beam movement along the vertical axis is neglected.

The described approximations were made for reasonable simplification of the method. In spite of the approximations, the method can be still considered to be reliable in comparison with the detector behavior in the real SEM. The future work should be addressed to the correction of the presented MTF and DQE characteristics for the specific SEMs instead of using the idealized case.

Nomenclature

CS	continual-sweep scan = scan with e-beam deflected by ramp part of sawtooth waveform
$\chi_{[a,\ b)}$	indicator function = function having value 1 in interval $[a, b)$ and the value 0 not in this interval
DQE	detective quantum efficiency
f	temporal frequency (Hz)
FT	Fourier transform
G	detector gain
i_{in}	detector input signal = signal incoming from object to detector (pA)
i_{out}	detector output signal = signal outgoing from detector (nA)
I_{in}	Fourier transform of i_{in} (pA)
I_{out}	Fourier transform of i_{out} (nA)
λ	distance in object plane corresponding to one pixel (nm)
MTF	modulation transfer function
NPS_{in}	input noise power spectrum = quadrate of Fourier transform of uniform i_{in} (pA^2)
NPS_{out}	output noise power spectrum = quadrate of Fourier transform of uniform i_{out} (nA^2)
o	intensity distribution of reflected/emitted electrons from object
p	e-beam current distribution (pA)
PBP	point-by-point scan = scan with e-beam deflected by staircase waveform
r	detector response function
s	spatial frequency = number of alternations from black line to white line per image distance (lp/pixel)
SNR	signal-to-noise ratio
t	time (ns)
τ	dwell time = time corresponding to period of one pixel integration (ns)
x	distance along horizontal axis (nm)

Acknowledgments

The authors thank the company CRYTUR, Ltd. for the supply of the single crystal scintillators. They also thank Luděk Frank (ISI AS CR, v.v.i.) for inspiring ideas and Milan Matějka (ISI AS CR, v.v.i.) for help with the experimental setup.

References

Bok J, Schauer P. 2011. LabVIEW-based control and data acquisition system for cathodoluminescence experiments. Rev Sci Instrum 82:113109.

Boreman GD. 2001. Modulation transfer fuction in optical and electro-optical systems. Bellingham, Washington: SPIE.

Bracewell RN. 1999. The Fourier transform and its applications. Singapore: McGraw-Hill.

Browne MT, Ward JFL. 1982. Detectors for STEM, and the measurement of their detective quantum efficiency. Ultramicroscopy 7:249–262.

Cunningham IA, Shaw R. 1999. Signal-to-noise optimization of medical imaging systems. J Opt Soc Am A 16:621–632.

Danov K, Danev R, Nagayama K. 2000. Electric charging of thin films measured using the contrast transfer function. Ultramicroscopy 87:45–54.

Everhart TE, Thornley RFM. 1960. Wide-band detector for micro-microampere low-energy electron currents. J Sci Instrum 37:246.

Faruqi AR, Henderson R. 2007. Electronic detectors for electron microscopy. Curr Opin Struct Biol 17:549–555.

Griffin BJ. 2011. A comparison of conventional Everhart–Thornley style and in-lens secondary electron detectors—a further variable in scanning electron microscopy. Scanning 33:162–173.

Horacek M. 2005. Modulation transfer function and detective quantum efficiency of electron bombarded charge coupled device detector for low energy electrons. Rev Sci Instrum 76:093704.

Jones RC. 1959. The statistics of electron detection. Adv Electron Electron Opt 11:88–108.

Joy DC, Joy CS, Bunn RD. 1996. Measuring the performance of scanning electron microscope detectors. Scanning 18:533–538.

Joy DC, Michael J, Griffin B. 2010. Evaluating SEM performance from the contrast transfer function. Metrology, inspection, and process control for microlithography XXIV, 76383J.

Mallick SP, Carragher B, Potter CS, *et al*. 2005. ACE: automated CTF estimation. Ultramicroscopy 104:8–29.

McMullan G, Faruqi AR, Henderson R, *et al*. 2009a. Experimental observation of the improvement in MTF from backthinning a CMOS direct electron detector. Ultramicroscopy 109:1144–1147.

McMullan G, Chen S, Henderson R, *et al*. 2009b. Detective quantum efficiency of electron area detectors in electron microscopy. Ultramicroscopy 109:1126–1143.

Meyer RR, Kirkland AI. 2000. Characterisation of the signal and noise transfer of CCD cameras for electron detection. Microsc Res Techn 49:269–280.

Milazzo A-C, Moldovan G, Lanman J, *et al*. 2010. Characterization of a direct detection device imaging camera for transmission electron microscopy. Ultramicroscopy 110:741–744.

Mitome M. 1999. Contrast transfer function under convergent beam illumination measured by field emission gun. J Electron Microsc 48:27–32.

Novák L, Müllerová I. 2009. Single electron response of the scintillator-light guide-photomultiplier detector. J Microsc 233:76–83.

Oatley CW. 2004. The detective quantum efficiency of the scintillator/photomultiplier in the scanning electron microscope. Advances in imaging and electron physics. Vol. 180 Amsterdam: Elsevier.

Pavan P, Zanella G, Zannoni R, *et al*. 1993. Spatial resolution in X-ray imaging with scintillating glass optical fiber plates. Nucl Instrum Meth A 327:600–604.

Pratt WK. 2006. Digital image processing. New York: John Wiley & Sons.

Schauer P. 2011. Optimization of decay kinetics of YAG:Ce single crystal scintillators for S(T)EM electron detectors. Nucl Instrum Meth B 269:2572–2577.

Sorzano COS, Jonic S, Núñez-Ramírez R, *et al*. 2007. Fast, robust, and accurate determination of transmission electron microscopy contrast transfer function. J Struct Biol 160:249–262.

Taniyama A, Oikawa T, Shindo D. 1997. Detective quantum efficiency of the 25 mum pixel size imaging plate for

transmission electron microscopes. J Electron Microsc 46:303–310.

Unser M, Trus BL, Steven AC. 1987. A new resolution criterion based on spectral signal-to-noise ratios. Ultramicroscopy 23:39–51.

Van Zwet EJ, Zandbergen HW. 1996. Measurement of the modulation transfer function of a slow-scan CCD camera on a TEM using a thin amorphous film as test signal. Ultramicroscopy 64:49–55.

Williams T. 1998. The optical transfer function of imaging systems. Bristol, England: Taylor & Francis.

Zuo JM. 1996. Electron detection characteristics of slow-scan CCD camera. Ultramicroscopy 66:21–33.